5-1978

Acoustic Imaging of Joined Surfaces

C. S. Tsai
Carnegie-Mellon University

S. K. Wang
Carnegie-Mellon University

C. C. Lee
Carnegie-Mellon University

Acoustic Imaging of Joined Surfaces

Abstract
In this paper, the results of imaging experiments with the interfacial region~ of representative solid material joints, using a transmission-type scanning acoustic microscope operating at 150 MHz, are reported. Voids and flaws in specially made joints as well as production-line silicon solder bonds (die bonded headers) have been detected using the transmission-mode of operation of the microscope. Acoustic velocity of epoxy in an organic adhesive bond has also been measured using a combination of transmission and interference-mode of operation.

Keywords
Nondestructive Evaluation

Disciplines
Materials Science and Engineering

ACOUSTIC IMAGING OF JOINED SURFACES

C. S. Tsai, S. K. Wang, and C. C. Lee
Center for the Joining of Materials

and

Department of Electrical Engineering
Carnegie-Mellon University
Pittsburgh, Pa. 15213

ABSTRACT

In this paper, the results of imaging experiments with the interfacial regions of representative solid material joints, using a transmission-type scanning acoustic microscope operating at 150 MHz, are reported. Voids and flaws in specially made joints as well as production-line silicon solder bonds (die bonded headers) have been detected using the transmission-mode of operation of the microscope. Acoustic velocity of epoxy in an organic adhesive bond has also been measured using a combination of transmission- and interference-mode of operation.

Introduction

The characteristics and strength of solid material joints, bonds, or composites are, to a large degree, influenced by the elastic properties of their interfacial regions such as stress distributions, microstructures, defects, voids, etc. It is thus desirable to visualize and ultimately characterize their interfacial regions using acoustic techniques[1]. A number of acoustic techniques capable of spatial resolution in the micron range have been developed in recent years[2-8], and some of them have been employed for the study of fracture and stress distribution in a single material[9,10]. We have employed a transmission-type scanning acoustic microscope[5] to image the interfacial regions of representative joints[11].

Key Components of the Transmission-Type Scanning Acoustic Microscope

The acoustic microscope consists essentially of an acoustic generator, two acoustic lenses, water cell, precision sample holder, mechanical scanning system, acoustic detector, signal processing electronics and storage CRT (Fig. 1). The acoustic waves are generated by a $LiNbO_3$ wafer transducer to which one end face of a sapphire rod is bonded. A spherical acoustic lens at the other end face of this rod allows the acoustic energy to be focused to a diffraction-limited spot. The focused acoustic beam is then reflected, refracted, scattered and attenuated at boundaries in the sample where variations in the elastic parameters occur. A second sapphire rod with an identical acoustic lens formed at one end face collects the transmitted acoustic energy. Another $LiNbO_3$ transducer bonded to the other end of this second sapphire rod converts the transmitted wave into an electrical signal which, after signal processing using a superheterodyne receiver, is fed to the CRT, resulting in an intensity-modulated image. By scanning the sample both laterally (in raster scan) and in depth, focused acoustic images for any cross section of the sample can be displayed on the CRT, and elastic inhomogenities in the sample mapped.

Figures 2 and 3 show, respectively, the photographs of the close-up and the whole set-up of the microscope.

Capabilities of the Acoustic Microscope

The key parameters of the acoustic microscope employed in this study are listed as follows:

- Spatial Resolution: 10 μm in water at 150 MHz
- Field of View for the Sample: 3x4 mm
- Magnification of Acoustic Images: 35
- Total Electrical Throughput Loss: 35 db
- Dynamic Range: 30 to 50 db at 1 mw (0dbm) input electric power, depending on the sample that has been examined
- Modes of Operation: Transmission mode and interference mode

The resolution capability of the microscope is demonstrated in the acoustic image of a 1000 mesh (25 μm periodicity and 10 μm thickness) copper grid which was inserted in the focal region of the acoustic beam in the water cell (see Fig. 4). Note that the bright areas correspond to larger transmission of acoustic energy and thus to the holes in the grid. Clearly, this microscope is capable of a spatial resolution of better than 10 μm in water at 150 MHz.

Acoustic Images of Solid Material Joints

A number of representative solid material joints, bonds, and composites have been examined using the transmission-mode and/or the interference-mode of operation. Some of the acoustic images that have been obtained are given in this paper. Additional acoustic images may be found in Ref. 11. Figures 5-7 and Fig. 8(a) show the acoustic images obtained using the transmission-mode of operation.

In the first specimen, a 400 mesh copper grid (2.5 mil periodicity and 1.75 mil thickness) was inserted between two brass sheets, each 2 mil thick, and glued into a composite using adhesive loctite 04E. The copper grid alone was first imaged and the resulting acoustic micrograph is shown in Fig. 5(a). Again, the bright areas correspond to the holes in the grid. A comparison of Fig. 5(a) with the optical image (not shown) indicates that the quality of the acoustic image is only slightly lower than that of the optical image. The acoustic micrograph for the composite is shown in Fig. 5(b). We see that some of the

bright areas have been lost, indicating that some debonding had occurred. We also note that the sizes of the bright areas are somewhat smaller than that of Fig. 5(a). This may possibly result from the imperfect contact at the edges of the holes and/or the effect of the adhesive through acoustic scattering. Thus, this particular specimen and the acoustic micrograph obtained serve to demonstrate that the acoustic microscope is capable of visualizing and detecting debonds of relatively thick joints/composites, consisting of both metallic and organic materials.

In the second specimen, a patch of epoxy was attached between two brass sheets, each 6 mil thick. In order to create a well defined variation in the thickness of the epoxy layer a fine metal wire was first laid at one end of the brass sheet to act as an uneven spacer before the epoxy has been applied. The acoustic micrograph obtained for the resulting bond is shown in Fig. 6. The dark dots in the image have been identified as resulting from the bonding flaws (in the form of air bubbles), and the fringe pattern as resulting from multiple acoustic reflections from the specimen. The first observation is confirmed by examination under an optical microscope after one of the brass sheets has been peeled off and the second observation is in agreement with the actual variation in the thickness of the epoxy layer as measured by a micrometer, namely, from 1.5 mils at one end to 4.5 mils at the other. Again, as in the first specimen, this particular bond and the acoustic micrograph obtained have clearly demonstrated the usefulness of the acoustic microscope for the inspection, identification and characterization of solid material bonds.

In the third specimen, a Motorola production-line die bonded header which consists of a 2.5x2.5 mm silicon wafer, Au-Sn solder and a copper plate as first polished to a suitable thickness from both end faces. The final thickness of the silicon wafer is 0.1 mm and that of the copper plate is 0.3 mm. The acoustic micrograph for the resulting bond is shown in Fig. 7. By scanning the specimen in depth it was found that the dark dots in the image reached the highest degree of focus as the focal region of the acoustic beam was brought to coincide with the solder region. Thus, it is concluded that the dark dots correspond to some voids in the bond. This particular bond and the acoustic micrograph obtained have clearly demonstrated that this acoustic microscope can be used to nondestructively observe voids in the semiconductor die bonds, one of the backbones of solid state electronics.

Note that the acoustic images shown in Figs. 4-7 were obtained using the transmission-mode of operation and, therefore, carry only amplitude information. However, phase information resulting from variations in the acoustic wave velocity and/or the thickness of the specimen is also important. For example, the strength of adhesive bonds have been shown to be closely related to the acoustic wave velocity of the adhesive[12]. We have employed a combination of the transmission-mode and the interference-mode of operation to measure the acoustic wave velocity of epoxy in a brass-epoxy-brass bond. In the interference-mode of operation the relative phase of the acoustic signals transmitted through the bond was obtained by comparing it with the phase of a reference electrical signal. Assuming that both brass plates are of uniform thickness and homogeneous in elastic parameters, we note that the relative phase of the transmitted acoustic signals is determined by the variation in the thickness of the epoxy layer and the acoustic velocities of both epoxy and water. Under this assumption, we see first that variation in the thickness of the epoxy layer is contained in the fringe pattern of the acoustic image obtained using the transmission-mode of operation. Next, the relative phase of the transmitted acoustic signals is contained in the fringe pattern of the acoustic image obtained using the interference-mode of operation. Thus, it is possible to deduce the acoustic wave velocity of the epoxy by counting the fringes in both acoustic images. The acoustic images obtained using the two modes of operation (for the same region of the brass-epoxy-brass bond) are shown in Fig. 8. By studying the fringe patterns in the acoustic images we have arrived at an acoustic wave velocity of 2.7×10^5 cm/sec for the epoxy in the bond. This measured value is in good agreement with the published data[12]. It is to be noted that spatial variation in the acoustic velocity may be determined by simply scanning the bond.

Conclusion

We have shown that the scanning acoustic microscope, operating in the transmission-mode of operation, is capable of detecting voids, flaws and defects in the interfacial regions of specially made joints/composites/bonds as well as production-line silicon solder bonds. We have also shown that the same microscope, when operating at a combination of transmission- and interference-mode of operation, can be used to measure the velocity of acoustic wave propagation in the bonding layer. Clearly, for each particular joint, bond or composite, more comprehensive study in which the individual parameter is independently controlled, is required to achieve a more detailed characterization.

Acknowledgements

We wish to thank Dr. E. Philofsky of Motorola for furnishing us the die bonded headers used in this study. Support from the Materials Research Laboratory Section, National Science Foundation, under Grant No. DMR72-03297-A03 is also gratefully acknowledged. S. K. Wang was also supported by an IBM Post Doctoral Fellowship.

References

1. See, for example, IEEE Trans. Sonics & Ultrasonics, Special Issue on Nondestructive Evaluation, SU-23, 283-374 (Sept 1976), Edited by D. O. Thompson.

2. L. W. Kessler, "Review of Progress and Applications in Acoustic Microscopy," (A) J. Acoust. Soc. Amer., 55, 909 (May 1974).

3. A. Korpel, L. W. Kessler, and P. R. Palermo, "An Acoustic Microscope Operating at 100 MHz," Nature, 232, 110 (1971).

4. B. A. Auld, R. J. Gilbert, K. Hyllested, C. G. Roberts, and D. C. Webb, "A 1.1 GHz Scanned Acoustic Microscope," Acoustical Holography, edited by G. Wade (Plenum, N.Y., 1972), 4, 73.

5. R. A. Lemons and C. F. Quate, "Acoustic Microscope-Scanning Version," Appl. Phys. Lett., 24, 163 (Feb. 1974).

6. R. A. Lemons and C. F. Quate, "Integrated Circuits as Viewed with an Acoustic Microscope," Appl. Phys. Lett., 25, 251 (Sept. 1974).

7. W. L. Bond, C. C. Cutler, R. A. Lemons, and C. F. Quate, "Dark-field and Stereo Viewing with the Acoustic Microscope," Appl. Phys. Lett., 27, 270 (Sept. 1975).

8. R. Kompfner and R. A. Lemons, "Nonlinear Acoustic Microscopy," Appl. Phys. Lett., 28, 295 (March 1976).

9. A. Madeyski and L. W. Kessler, "Initial Experiments in the Application of Acoustic Microscopy to the Characterization of Steel and to the Study of Fracture Phenomena," IEEE Trans. Sonics & Ultrasonics, SU-23, 373 (Sept. 1976).

10. J. Souquet and G. S. Kino, "Acoustic Phase Technique for Measuring Stress Region in Materials," 1976 Ultrasonics Symposium Proceedings, IEEE Cat. #76 CH1120-5SU, 582

11. C. S. Tsai, S. K. Wang, and C. C. Lee, "Visualization of Solid Material Joints Using a Transmission-Type Scanning Acoustic Microscope," to appear in Appl. Phys. Lett., (Aug. 1977).

12. G. A. Alers, P. L. Flynn, and M. J. Buckley, "Ultrasonic Techniques for Measuring the Strength of Adhesive Bonds," Materials Evaluation, 35, No. 4, 77-84 (April 1977).

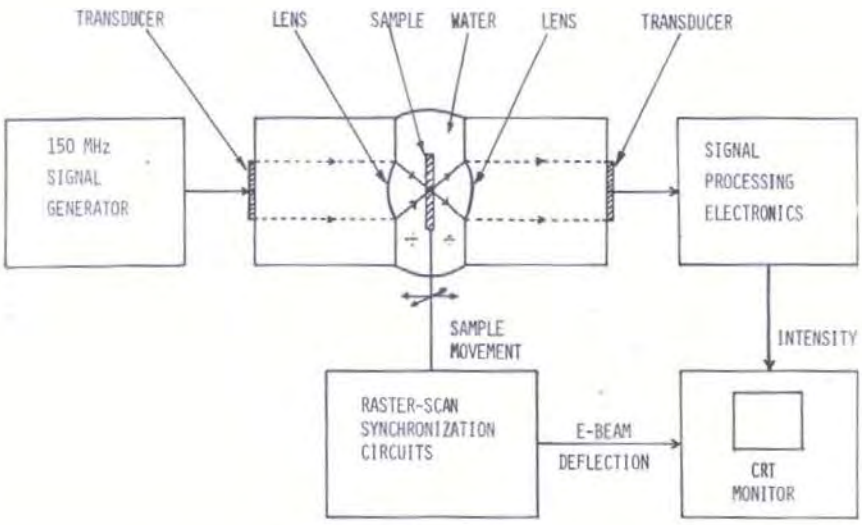

Figure 1. Block diagram.

Figure 2. Photograph of the acoustic microscope (the close-up).

Figure 3. Photograph of the acoustic microscope (the whole setup).

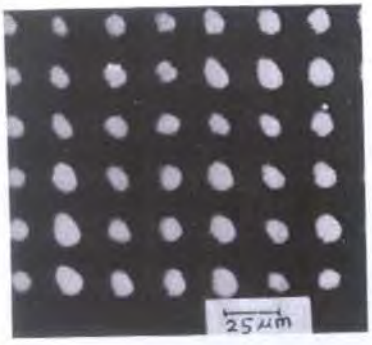

Figure 4. Acoustic image of a 1000-mesh copper grid (25 μm periodicity and 10 μm thickness).

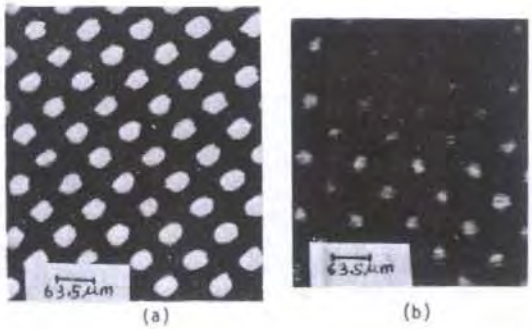

(a) (b)

Figure 5. (a) Acoustic image of a 400-mesh copper grid (62.5 μm periodicity and 44 μm thickness). (b) Acoustic image of a brass-copper grid-adhesive-brass joint (the copper grid is that of (a), thickness of each brass sheet is 2 mils).

Figure 6. Acoustic image of a brass-epoxy-brass joint (thickness of each brass sheet is 6 mils, thickness of epoxy layer varies from 1.5 mils at one end to 4.5 mils at the other).

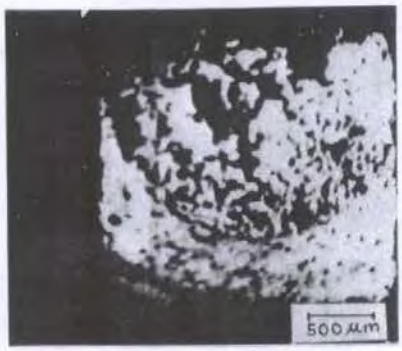

Figure 7. Acoustic images of solder bonds of silicon on copper. (Motorola production-line die bonded headers. The solder is Au-Sn preform; silicon dimensions are 2.5 x 2.5 x 0.1 mm; copper header is 0.3 mm thick).

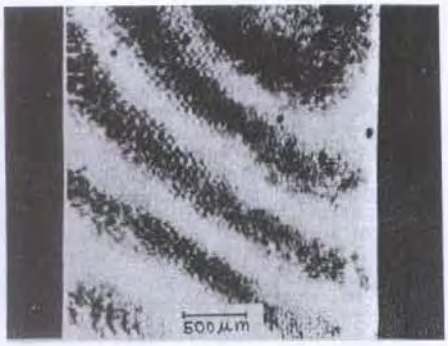

(a)

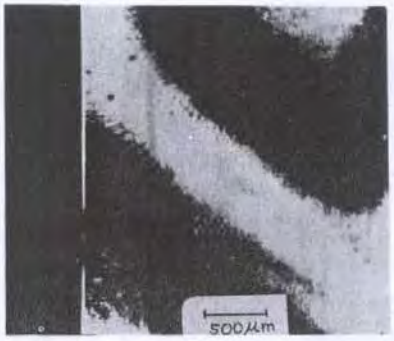

(b)

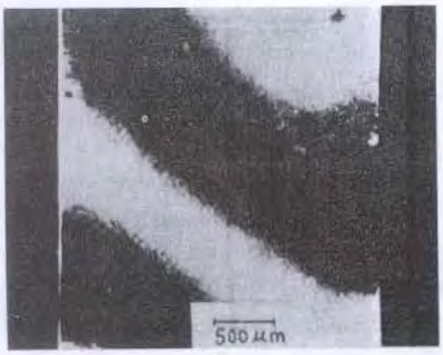

(c)

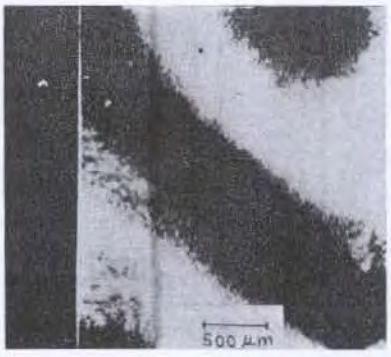

(d)

Figure 8. Acoustic images of brass-epoxy-brass bond (thickness of each brass sheet is 4 mils and that of epoxy layer is 1.0 mil).

(a) Acoustic image obtained using transmission-mode of operation.
(b) Acoustic image obtained using interference-mode of operation.
(c) Same as in (b), but with a change in phase reference by 90°.
(d) Same as in (b), but with a change in phase reference by 180°.